**Chapter 9: Commonly Used Models: Narrow-Band Gaussian Noise and Shot Noise**

Narrow-band, wide-sense-stationary (WSS) Gaussian noise $\eta(t)$ is used often as a noise model in communication systems. For example, $\eta(t)$ might be the noise component in the output of a radio receiver intermediate frequency (*IF*) filter/amplifier. In these applications, sample functions of $\eta(t)$ are expressed as

$$\eta(t) = \eta_c(t)\cos\omega_c t - \eta_s(t)\sin\omega_c t\,, \tag{9-1}$$

where $\omega_c$ is termed the *center frequency* (for example, $\omega_c$ could be the actual center frequency of the above-mentioned *IF* filter). The quantities $\eta_c(t)$ and $\eta_s(t)$ are termed the *quadrature components* (sometimes, $\eta_c(t)$ is known as the *in-phase* component and $\eta_s(t)$ is termed the *quadrature* component), and they are assumed to be real-valued.

Narrow-band noise $\eta(t)$ can be represented in terms of its *envelope* R(t) and *phase* $\phi(t)$. This representation is given as

$$\eta(t) = R(t)\cos(\omega_c t + \phi(t))\,, \tag{9-2}$$

where

$$\begin{aligned} R(t) &\equiv \sqrt{\eta_c^2(t) + \eta_s^2(t)} \\ \phi(t) &\equiv \tan^{-1}(\eta_s(t)/\eta_c(t)). \end{aligned} \tag{9-3}$$

Normally, it is assumed that $R(t) \geq 0$ and $-\pi < \phi(t) \leq \pi$ for all time.

Note the initial assumptions placed on $\eta(t)$. The assumptions of Gaussian and WSS behavior are easily understood. The narrow-band attribute of $\eta(t)$ means that $\eta_c(t)$, $\eta_s(t)$, R(t) and $\phi(t)$ are low-pass processes; these low-pass processes vary slowly compared to $\cos\omega_c t$; they

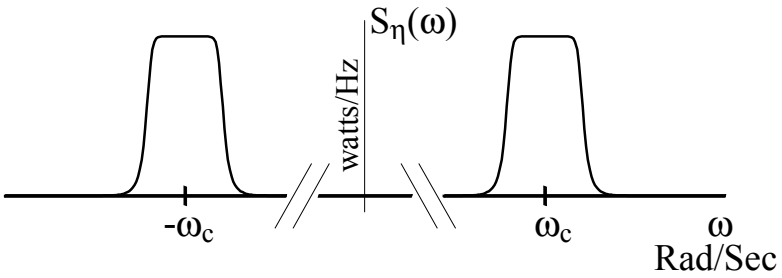


**Fig. 9-1:** Example spectrum of narrow-band noise.

are on a vastly different time scale from $\cos\omega_c t$. Many periods of $\cos\omega_c t$ occur before there is notable change in $\eta_c(t)$, $\eta_s(t)$, R(t) or $\phi(t)$.

A second interpretation can be given for the term *narrow-band*. This is accomplished in terms of the power spectrum of $\eta(t)$, denoted as $\mathcal{S}_\eta(\omega)$. By the Wiener-Khinchine theorem, $\mathcal{S}_\eta(\omega)$ is the Fourier transform of $R_\eta(\tau)$, the autocorrelation function for WSS $\eta(t)$. Since $\eta(t)$ is real valued, the spectral density $\mathcal{S}_\eta(\omega)$ satisfies

$$\begin{aligned} &\mathcal{S}_\eta(\omega) \geq 0 \\ &\mathcal{S}_\eta(\omega) = \mathcal{S}_\eta(-\omega). \end{aligned} \tag{9-4}$$

Figure 9-1 depicts an example spectrum of a narrow-band process. The *narrow-band* attribute means that $\mathcal{S}_\eta(\omega)$ is zero except for a narrow band of frequencies around $\pm\omega_c$; process $\eta(t)$ has a bandwidth (however it might be defined) that is small compared to the center frequency $\omega_c$.

Power spectrum $\mathcal{S}_\eta(\omega)$ **may, or may not**, have $\pm\omega_c$ as axes of **local symmetry**. *If* $\omega_c$ is an axis of local symmetry, then

$$\mathcal{S}_\eta(\omega + \omega_c) = \mathcal{S}_\eta(-\omega + \omega_c) \tag{9-5}$$

for $0 < \omega < \omega_c$, and the process is said to be a *symmetrical band-pass process* (Fig. 9-1 depicts a symmetrical band-pass process). It must be emphasized that the symmetry stated by the second of (9-4) is always true (*i.e.,* the power spectrum is even); however, the symmetry stated by (9-5)

may, or may not, be true. As will be shown in what follows, the analysis of narrow-band noise is simplified *if* (9-5) is true.

To avoid confusion when reviewing the engineering literature on narrow-band noise, the reader should remember that different authors use slightly different definitions for the cross-correlation of jointly-stationary, real-valued random processes x(t) and y(t). As used here, the cross-correlation of x and y is defined as $R_{xy}(\tau) \equiv E[x(t+\tau)y(t)]$. However, when defining $R_{xy}$, some authors shift (by $\tau$) the time variable of the function y instead of the function x. Fortunately, this possible discrepancy is accounted for easily when comparing the work of different authors.

**$\eta(t)$ has Zero Mean**

The mean of $\eta(t)$ must be zero. This conclusion follows directly from

$$E[\eta(t)] = E[\eta_c(t)]\cos\omega_c t - E[\eta_s(t)]\sin\omega_c t . \tag{9-6}$$

The WSS assumption means that $E[\eta(t)]$ must be time invariant (constant). Inspection of (9-6) leads to the conclusion that $E[\eta_c] = E[\eta_s] = 0$ so that $E[\eta] = 0$.

**Quadrature Components In Terms of $\eta$ and $\hat{\eta}$**

Let the Hilbert transform of WSS noise $\eta(t)$ be denoted in the usual way by the use of a circumflex; that is, $\hat{\eta}(t)$ denotes the Hilbert transform of $\eta(t)$ (see Appendix 9A for a discussion of the Hilbert transform). The Hilbert transform is a linear, time-invariant filtering operation applied to $\eta(t)$; hence, from the results developed in Chapter 7, $\hat{\eta}(t)$ is WSS.

In what follows, some simple properties are needed of the cross correlation of $\eta(t)$ and $\hat{\eta}(t)$. Recall that $\hat{\eta}(t)$ is the output of a linear, time-invariant system that is driven by $\eta(t)$. Also recall that techniques are given in Chapter 7 for expressing the cross correlation between a system input and output. Using this approach, it can be shown easily that

$$R_{\eta\hat{\eta}}(\tau) \equiv E[\eta(t+\tau)\hat{\eta}(t)] = -\hat{R}_{\eta}(\tau)$$

$$R_{\hat{\eta}\eta}(\tau) \equiv E[\hat{\eta}(t+\tau)\eta(t)] = \hat{R}_{\eta}(\tau) \qquad (9\text{-}7)$$

$$R_{\hat{\eta}\eta}(0) = R_{\eta\hat{\eta}}(0) = 0$$

$$R_{\hat{\eta}}(\tau) = R_{\eta}(\tau) .$$

Equation (9-1) can be used to express $\hat{\eta}(t)$. The Hilbert transform of the noise signal can be expressed as

$$\hat{\eta}(t) = \widehat{\eta_c(t)\cos\omega_c t - \eta_s(t)\sin\omega_c t} = \eta_c(t)\widehat{\cos\omega_c t} - \eta_s(t)\widehat{\sin\omega_c t} \qquad (9\text{-}8)$$

$$= \eta_c(t)\sin\omega_c t + \eta_s(t)\cos\omega_c t .$$

This result follows from the fact that $\omega_c$ is much higher than any frequency component in $\eta_c$ or $\eta_s$ so that the Hilbert transform is only applied to the high-frequency sinusoidal functions (see Appendix 9A).

The quadrature components can be expressed in terms of $\eta$ and $\hat{\eta}$. This can be done by solving (9-1) and (9-8) for

$$\eta_c(t) = \eta(t)\cos\omega_c t + \hat{\eta}(t)\sin\omega_c t$$

$$\eta_s(t) = \hat{\eta}(t)\cos\omega_c t - \eta(t)\sin\omega_c t . \qquad (9\text{-}9)$$

These equations express the quadrature components as a linear combination of Gaussian $\eta$. Hence, the components $\eta_c$ and $\eta_s$ are Gaussian. In what follows, Equation (9-9) will be used to calculate the autocorrelation and crosscorrelation functions of the quadrature components. It will be shown that the quadrature components are WSS and that $\eta_c$ and $\eta_s$ are jointly WSS. Furthermore, WSS process $\eta(t)$ is a symmetrical band-pass process if, and only if, $\eta_c$ and $\eta_s$ are

uncorrelated for all time shifts.

**Relationships Between Autocorrelation Functions $R_\eta$, $R_{\eta_c}$ and $R_{\eta_s}$**

It is easy to compute, in terms of $R_\eta$, the autocorrelation of the quadrature components. Use (9-9) and compute the autocorrelation

$$\begin{aligned} R_{\eta_c}(\tau) &= E[\eta_c(t)\eta_c(t+\tau)] \\ &= E[\eta(t)\eta(t+\tau)]\cos\omega_c t\cos\omega_c(t+\tau) + E[\hat{\eta}(t)\eta(t+\tau)]\sin\omega_c t\cos\omega_c(t+\tau) \\ &\quad + E[\eta(t)\hat{\eta}(t+\tau)]\cos\omega_c t\,\sin\omega_c(t+\tau) + E[\hat{\eta}(t)\hat{\eta}(t+\tau)]\sin\omega_c t\,\sin\omega_c(t+\tau). \end{aligned} \tag{9-10}$$

This last result can be simplified by using (9-7) to obtain

$$\begin{aligned} R_{\eta_c}(\tau) &= R_\eta(\tau)[\cos\omega_c t\cos\omega_c(t+\tau) + \sin\omega_c t\,\sin\omega_c(t+\tau)] \\ &\quad + \hat{R}_\eta(\tau)[\cos\omega_c t\,\sin\omega_c(t+\tau) - \sin\omega_c t\,\cos\omega_c(t+\tau)], \end{aligned}$$

a result that can be expressed as

$$R_{\eta_c}(\tau) = R_\eta(\tau)\cos\omega_c\tau + \hat{R}_\eta(\tau)\sin\omega_c\tau. \tag{9-11}$$

The same procedure can be used to compute an identical result for $R_{\eta_s}$; this leads to the conclusion that

$$R_{\eta_c}(\tau) \equiv R_{\eta_s}(\tau) \tag{9-12}$$

for all $\tau$.

A somewhat non-intuitive result can be obtained from (9-11) and (9-12). Set $\tau = 0$ in the last two equations to conclude that

$$R_\eta(0) = R_{\eta_c}(0) = R_{\eta_s}(0), \tag{9-13}$$

an observation that leads to

$$\begin{aligned} &E[\eta^2(t)] = E[\eta_c^2(t)] = E[\eta_s^2(t)] \\ &\text{Avg Pwr in } \eta(t) = \text{Avg Pwr in } \eta_c(t) = \text{Avg Pwr in } \eta_s(t). \end{aligned} \tag{9-14}$$

The frequency domain counterpart of (9-11) relates the spectrums $\mathcal{S}_\eta$, $\mathcal{S}_{\eta_c}$ and $\mathcal{S}_{\eta_s}$. Take the Fourier transform of (9-11) to obtain

$$\begin{aligned} \mathcal{S}_{\eta_c}(\omega) = \mathcal{S}_{\eta_s}(\omega) &= \frac{1}{2}\left(\mathcal{S}_\eta(\omega+\omega_c) + \mathcal{S}_\eta(\omega-\omega_c)\right) \\ &\quad -\frac{1}{2}\left(\text{sgn}(\omega-\omega_c)\mathcal{S}_\eta(\omega-\omega_c) - \text{sgn}(\omega+\omega_c)\mathcal{S}_\eta(\omega+\omega_c)\right). \end{aligned} \tag{9-15}$$

Since $\eta_c$ and $\eta_s$ are low-pass processes, Equation (9-15) can be simplified to produce

$$\begin{aligned} \mathcal{S}_{\eta_c}(\omega) = \mathcal{S}_{\eta_s}(\omega) &= \mathcal{S}_\eta(\omega+\omega_c) + \mathcal{S}_\eta(\omega-\omega_c), \quad -\omega_c \le \omega \le \omega_c \\ &= 0, \qquad\qquad\qquad\qquad \text{otherwise,} \end{aligned} \tag{9-16}$$

a relationship that is easier to grasp and remember than is (9-11).

Equation (9-16) provides an easy method for obtaining $\mathcal{S}_{\eta_c}$ and/or $\mathcal{S}_{\eta_s}$ given only $\mathcal{S}_\eta$. First, make two copies of $\mathcal{S}_\eta(\omega)$. Shift the first copy to the left by $\omega_c$, and shift the second copy to the right by $\omega_c$. Add together both shifted copies, and truncate the sum to the interval $-\omega_c \le \omega \le \omega_c$ to get $\mathcal{S}_{\eta_c}$. This "shift and add" procedure for creating $\mathcal{S}_{\eta_c}$ is illustrated by Fig. 9-2. Given only $\mathcal{S}_\eta(\omega)$, it is *always* possible to determine $\mathcal{S}_{\eta_c}$ (which is equal to $\mathcal{S}_{\eta_s}$) in this manner. The converse is not true; given only $\mathcal{S}_{\eta_c}$, it is not always possible to create $\mathcal{S}_\eta(\omega)$ (Why? Think

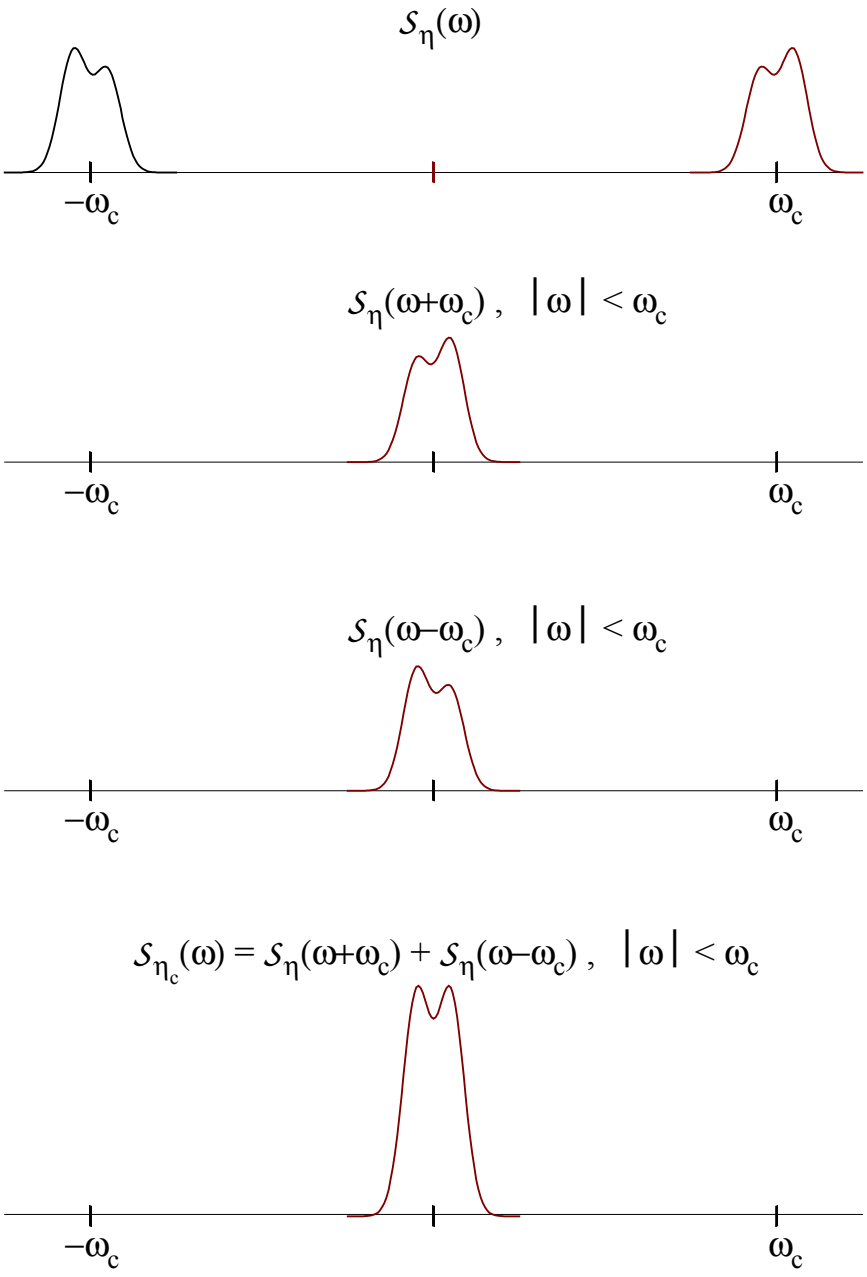


**Fig. 9-2:** Creation of $S_{\eta_c}$ from shifting and adding copies of $S_\eta$.

about the fact that $S_{\eta_c}(\omega)$ must be even, but $S_\eta(\omega)$ may not satisfy (9-5)).

**The Crosscorrelation $R_{\eta_c\eta_s}$**

It is easy to compute the cross-correlation of the quadrature components. From (9-9) it follows that

$$R_{\eta_c\eta_s}(\tau) = E[\eta_c(t+\tau)\eta_s(t)]$$

$$= E[\eta(t+\tau)\hat{\eta}(t)]\cos\omega_c(t+\tau)\cos\omega_c t - E[\eta(t+\tau)\eta(t)]\cos\omega_c(t+\tau)\sin\omega_c t \qquad (9\text{-}17)$$

$$+ E[\hat{\eta}(t+\tau)\hat{\eta}(t)]\sin\omega_c(t+\tau)\cos\omega_c t - E[\hat{\eta}(t+\tau)\eta(t)]\sin\omega_c(t+\tau)\sin\omega_c t\ .$$

By using (9-7), Equation (9-17) can be simplified to obtain

$$R_{\eta_c\eta_s}(\tau) = R_\eta(\tau)[-\sin\omega_c t\cos\omega_c(t+\tau) + \cos\omega_c t\ \sin\omega_c(t+\tau)]$$

$$- \hat{R}_\eta(\tau)[\cos\omega_c t\ \cos\omega_c(t+\tau) + \sin\omega_c t\ \sin\omega_c(t+\tau)],$$

a result that can be written as

$$R_{\eta_c\eta_s}(\tau) = R_\eta(\tau)\sin\omega_c\tau - \hat{R}_\eta(\tau)\cos\omega_c\tau\ . \qquad (9\text{-}18)$$

The cross-correlation of the quadrature components is an odd function of $\tau$. This follows directly from inspection of (9-18) and the fact that an even function has an odd Hilbert transform. Finally, the fact that this cross-correlation is odd implies that $R_{\eta_c\eta_s}(0) = 0$; *taken at the same time, the samples of* $\eta_c$ *and* $\eta_s$ *are uncorrelated and independent*. However, as discussed below, the quadrature components $\eta_c(t_1)$ and $\eta_s(t_2)$ may be correlated for $t_1 \neq t_2$.

The autocorrelation $R_\eta$ of the narrow-band noise can be expressed in terms of the autocorrelation and cross-correlation of the quadrature components $\eta_c$ and $\eta_s$. This important result follows from using (9-11) and (9-18) in

$$R_{\eta_c}(\tau)\cos\omega_c\tau + R_{\eta_c\eta_s}(\tau)\sin\omega_c\tau = \left[R_\eta(\tau)\cos\omega_c\tau + \hat{R}_\eta(\tau)\sin\omega_c\tau\right]\cos\omega_c\tau$$

$$+\left[R_\eta(\tau)\sin\omega_c\tau - \hat{R}_\eta(\tau)\cos\omega_c\tau\right]\sin\omega_c\tau\ . \qquad (9\text{-}19)$$

However, $R_\eta$ results from simplification of the right hand side of (9-19), and the desired relationship

$$R_\eta(\tau) = R_{\eta_c}(\tau)\cos\omega_c\tau + R_{\eta_c\eta_s}(\tau)\sin\omega_c\tau \tag{9-20}$$

follows.

Comparison of (9-16) with the Fourier transform of (9-20) reveals an "unsymmetrical" aspect in the relationship between $\mathcal{S}_\eta$, $\mathcal{S}_{\eta_c}$ and $\mathcal{S}_{\eta_s}$. In *all* cases, both $\mathcal{S}_{\eta_c}$ and $\mathcal{S}_{\eta_s}$ can be obtained by *simple* translations of $\mathcal{S}_\eta$ as is shown by (9-16). However, *in general*, $\mathcal{S}_\eta$ cannot be expressed in terms of a similar, *simple* translation of $\mathcal{S}_{\eta_c}$ (or $\mathcal{S}_{\eta_s}$), a conclusion reached by inspection of the Fourier transform of (9-20). But, as shown next, there is an important special case where $R_{\eta_c\eta_s}(\tau)$ is identically zero for all $\tau$, and $\mathcal{S}_\eta$ can be expresses as simple translations of $\mathcal{S}_{\eta_c}$.

**Symmetrical Bandpass Processes**

Narrow-band process $\eta(t)$ is said to be a *symmetrical band-pass process* if

$$\mathcal{S}_\eta(\omega + \omega_c) = \mathcal{S}_\eta(-\omega + \omega_c) \tag{9-21}$$

for $0 < \omega < \omega_c$. Such a bandpass process has its center frequency $\omega_c$ as an axis of local symmetry. In nature, symmetry usually leads to simplifications, and this is true of Gaussian narrow-band noise. In what follows, we show that the local symmetry stated by (9-21) is equivalent to the condition $R_{\eta_c\eta_s}(\tau) = 0$ for *all* $\tau$ (not just at $\tau = 0$).

The desired result follows from inspecting the Fourier transform of (9-18); this transform is the cross spectrum of the quadrature components, and it vanishes when the narrow-band process has spectral symmetry as defined by (9-21). To compute this cross spectrum, first note the Fourier transform pairs

$$\begin{aligned} &R_\eta(\tau) \leftrightarrow \mathcal{S}_\eta(\omega) \\ &\hat{R}_\eta(\tau) \leftrightarrow -j\mathrm{Sgn}(\omega)\mathcal{S}_\eta(\omega), \end{aligned} \tag{9-22}$$

where

$$\mathrm{Sgn}(\omega) \equiv \begin{cases} +1 & \text{for } \omega > 0 \\ -1 & \text{for } \omega < 0 \end{cases} \tag{9-23}$$

is the commonly used "sign" function. Now, use Equation (9-22) and the Frequency Shifting Theorem to obtain the Fourier transform pairs

$$\begin{aligned} &R_\eta(\tau)\sin\omega_c\tau \leftrightarrow \frac{1}{2j}\left[\mathcal{S}_\eta(\omega-\omega_c) - \mathcal{S}_\eta(\omega+\omega_c)\right] \\ &\hat{R}_\eta(\tau)\cos\omega_c\tau \leftrightarrow \frac{1}{2j}\left[\mathrm{Sgn}(\omega-\omega_c)\mathcal{S}_\eta(\omega-\omega_c) + \mathrm{Sgn}(\omega+\omega_c)\mathcal{S}_\eta(\omega+\omega_c)\right]. \end{aligned} \tag{9-24}$$

Finally, use this last equation and (9-18) to compute the cross spectrum

$$\begin{aligned} \mathcal{S}_{\eta_c\eta_s}(\omega) &= \mathcal{F}[R_{\eta_c\eta_s}(\tau)] \\ &= \frac{1}{2j}\left[\mathcal{S}_\eta(\omega-\omega_c)[1-\mathrm{Sgn}(\omega-\omega_c)] - \mathcal{S}_\eta(\omega+\omega_c)[1+\mathrm{Sgn}(\omega+\omega_c)]\right]. \end{aligned} \tag{9-25}$$

Figure 9-3 depicts example plots useful for visualizing important properties of (9-25). From parts b) and c) of this plot, note that the products on the right-hand side of (9-25) are low pass processes. Then it is easily seen that

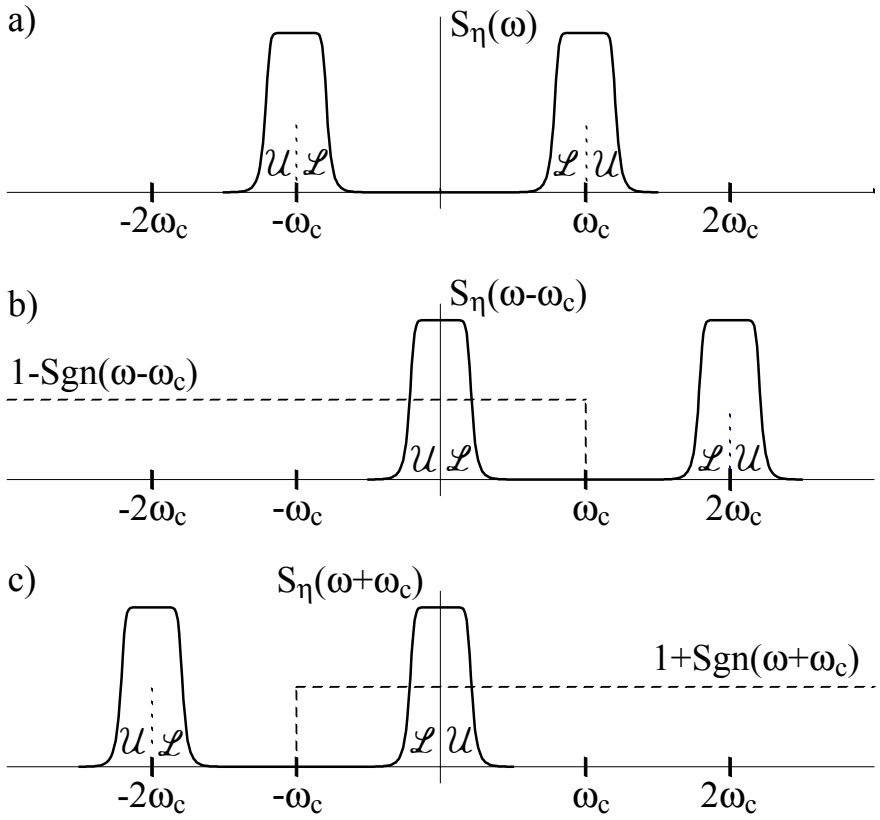


**Figure 9-3:** Symmetrical bandpass processes have $\eta_c(t_1)$ and $\eta_s(t_2)$ uncorrelated for all $t_1$ and $t_2$.

$$\mathcal{S}_{\eta_c\eta_s}(\omega)=\begin{cases}0, & \omega>\omega_c\\ -j[\mathcal{S}_\eta(\omega-\omega_c)-\mathcal{S}_\eta(\omega+\omega_c)], & -\omega_c<\omega<\omega_c\\ 0, & \omega<-\omega_c\,.\end{cases} \tag{9-26}$$

Finally, note that $\mathcal{S}_{\eta_c\eta_s}(\omega)=0$ is equivalent to the narrow-band process $\eta$ satisfying the symmetry condition (9-21). Since the cross spectrum is the Fourier transform of the cross-correlation, this last statement implies that, for *all* $t_1$ and $t_2$ (not just $t_1 = t_2$), $\eta_c(t_1)$ and $\eta_s(t_2)$ are uncorrelated if and only if (9-21) holds. On Fig. 9-3, symmetry implies that the spectral components labeled with $\mathcal{U}$ can be obtained from those labeled with $\mathcal{L}$ by a simple folding operation.

System analysis is simplified greatly if the noise encountered has a symmetrical

spectrum. Under these conditions, the quadrature components are uncorrelated, and (9-20) simplifies to

$$R_\eta(\tau) = R_{\eta_c}(\tau)\cos\omega_c\tau\,. \tag{9-27}$$

Also, the spectrum $\mathcal{S}_\eta$ of the noise is obtained easily by scaling and translating $\mathcal{S}_{\eta_c} \equiv \mathcal{F}[R_{\eta_c}]$ as shown by

$$\mathcal{S}_\eta(\omega) = \frac{1}{2}[\mathcal{S}_{\eta_c}(\omega-\omega_c) + \mathcal{S}_{\eta_c}(\omega+\omega_c)]. \tag{9-28}$$

This result follows directly by taking the Fourier transform of (9-27). Hence, when the process is symmetrical, it is possible to express $\mathcal{S}_\eta$ in terms of a *simple* translations of $\mathcal{S}_{\eta_c}$ (see the comment after (9-20)). Finally, for a symmetrical bandpass process, Equation (9-16) simplifies to

$$\begin{aligned} \mathcal{S}_{\eta_c}(\omega) \;=\; \mathcal{S}_{\eta_s}(\omega) \;&=\; 2\mathcal{S}_\eta(\omega+\omega_c), \quad -\omega_c \le \omega \le \omega_c \\ &=\; 0, \qquad\qquad \text{otherwise} \end{aligned}\,. \tag{9-29}$$

**Example 9-1:** Figure 9-4 depicts a simple RLC bandpass filter that is driven by white Gaussian noise with a double sided spectral density of $N_0/2$ watts/Hz. The spectral density of the output is

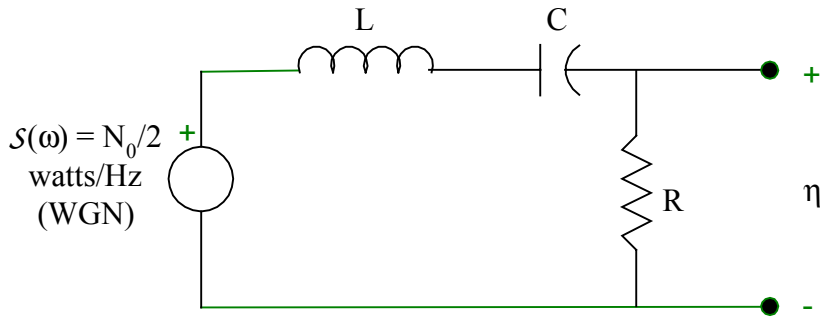


**Figure 9-4:** A simple band-pass filter driven by white Gaussian noise (WGN).

given by

$$\mathcal{S}_\eta(\omega) = \frac{N_0}{2}\left|H_{bp}(j\omega)\right|^2 = \frac{N_0}{2}\left|\frac{2\alpha_0(j\omega)}{(\alpha_0 + j\omega)^2 + \omega_c^2}\right|^2, \tag{9-30}$$

where $\alpha_0$ = R/2L, $\omega_c = (\omega_n^2 - \alpha_0^2)^{1/2}$ and $\omega_n = 1/(LC)^{1/2}$. In this result, frequency can be normalized, and (9-30) can be written as

$$\mathcal{S}_\eta(\omega') = \frac{N_0}{2}\left|\frac{2\alpha_0'(j\omega')}{(\alpha_0' + j\omega')^2 + 1}\right|^2, \tag{9-31}$$

where $\alpha_0' = \alpha_0/\omega_c$ and $\omega' = \omega/\omega_c$. Figure 9-5 illustrates a plot of the output spectrum for $\alpha_o' = .5$; note that the output process is not symmetrical. Figure 9-6 depicts the spectrum for $\alpha_o' = .1$ (a much "sharper" filter than the $\alpha_o' = .5$ case). As the circuit Q becomes large (*i.e.*, $\alpha_o'$ becomes small), the filter approximates a symmetrical filter, and the output process approximates a symmetrical bandpass process.

**Envelope and Phase of Narrow-Band Noise**

Zero-mean quadrature components $\eta_c(t)$ and $\eta_s(t)$ are jointly Gaussian, and they have the

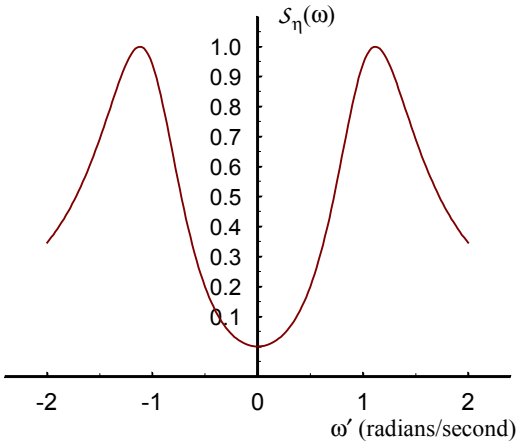


**Figure 9-5:** Output Spectrum for $\alpha_o' = .5$

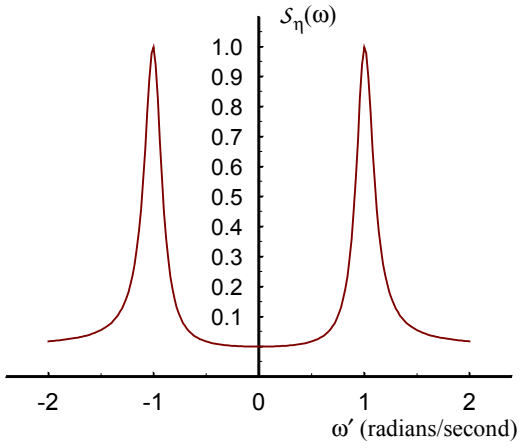


**Figure 9-6:** Output Spectrum for $\alpha_o' = .1$

same variance $\sigma^2 = R_\eta(0) = R_{\eta_c}(0) = R_{\eta_s}(0)$. Also, taken at the same time t, they are independent. Hence, taken at the same time, processes $\eta_c(t)$ and $\eta_s(t)$ are described by the joint density

$$f(\eta_c, \eta_s) = \frac{1}{2\pi\sigma^2} \exp\left[ -\frac{\eta_c^2 + \eta_s^2}{2\sigma^2} \right]. \tag{9-32}$$

We are guilty of a common abuse of notation. Here, symbols $\eta_c$ and $\eta_s$ are used to denote random processes, **and** sometimes they are used as algebraic variables, as in (9-32). However, always, it should be clear from context the intended use of $\eta_c$ and $\eta_s$.

The narrow-band noise signal can be represented as

$$\begin{aligned} \eta(t) &= \eta_c(t)\cos\omega_c t - \eta_s(t)\sin\omega_c t \\ &= \Gamma_1(t)\cos(\omega_c t + \varphi_1(t)) \end{aligned} \tag{9-33}$$

where

$$\begin{aligned} \Gamma_1(t) &= \sqrt{\eta_c^2(t) + \eta_s^2(t)} \\ \varphi_1(t) &= \mathrm{Tan}^{-1}\left( \frac{\eta_s(t)}{\eta_c(t)} \right), \ -\pi < \varphi_1 \le \pi, \end{aligned} \tag{9-34}$$

are the envelope and phase, respectively. Note that (9-34) describe a transformation of $\eta_c(t)$ and $\eta_s(t)$. The inverse is given by

$$\begin{aligned} \eta_c &= \Gamma_1 \cos(\varphi_1) \\ \eta_s &= \Gamma_1 \sin(\varphi_1) \end{aligned} \tag{9-35}$$

The joint density of $\Gamma_1$ and $\varphi_1$ can be found by using standard techniques. Since (9-35) is the inverse of (9-33) and (9-34), we can write

$$f(\Gamma_1,\varphi_1) = f(\eta_c,\eta_s)\left|\det\frac{\partial(\eta_c,\eta_s)}{\partial(\Gamma_1,\varphi_1)}\right|_{\substack{\eta_c=\Gamma_1\cos\varphi_1\\ \eta_s=\Gamma_1\sin\varphi_1}} \tag{9-36}$$

$$\frac{\partial(\eta_c,\eta_s)}{\partial(\Gamma_1,\varphi_1)} = \begin{bmatrix}\cos\varphi_1 & -\Gamma_1\sin\varphi_1\\ \sin\varphi_1 & \Gamma_1\cos\varphi_1\end{bmatrix}$$

(again, the notation is abusive). Finally, substitute (9-32) into (9-36) to obtain

$$\begin{aligned} f(\Gamma_1,\varphi_1) &= \frac{\Gamma_1}{2\pi\sigma^2}\exp\left[-\frac{1}{2\sigma^2}\Gamma_1{}^2(\sin^2\varphi_1+\cos^2\varphi_1)\right]\\ &= \frac{\Gamma_1}{2\pi\sigma^2}\exp\left[-\frac{1}{2\sigma^2}\Gamma_1{}^2\right], \end{aligned} \tag{9-37}$$

for $\Gamma_1 \ge 0$ and $-\pi < \varphi_1 \le \pi$. Finally, note that (9-37) can be represented as

$$f(\Gamma_1,\varphi_1) = f(\Gamma_1)f(\varphi_1), \tag{9-38}$$

where

$$f(\Gamma_1) = \frac{\Gamma_1}{\sigma^2}\exp\left[-\frac{1}{2\sigma^2}\Gamma_1{}^2\right]U(\Gamma_1) \tag{9-39}$$

describes a ***Rayleigh distributed envelope***, and

$$f(\varphi_1) = \frac{1}{2\pi}, \quad -\pi < \varphi_1 \le \pi \tag{9-40}$$

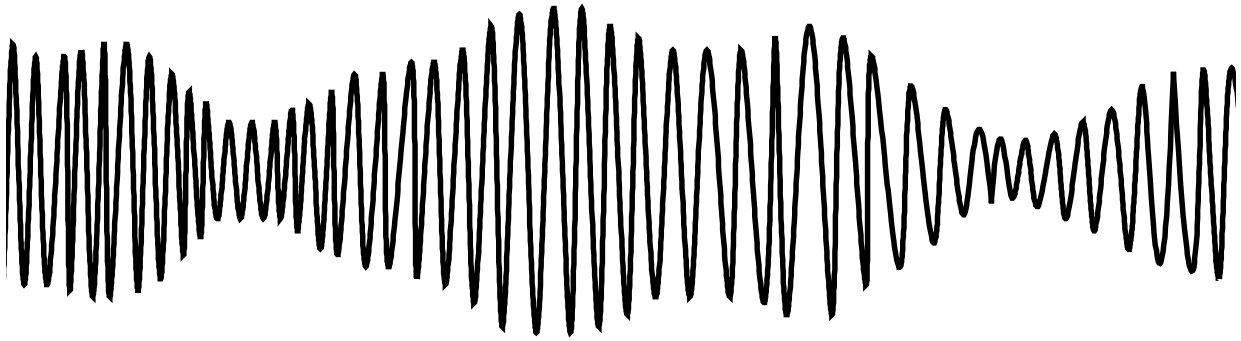

**Fig. 9-7:** A hypothetical sample function of narrow-band Gaussian noise. The envelope is Rayleigh and the phase is uniform.

describes a ***uniformly distributed phase***. Finally, note that the envelope and phase are independent. Figure 9-7 depicts a hypothetical sample function of narrow-band Gaussian noise.

**Envelope and Phase of a Sinusoidal Signal Plus Noise - the *Rice* Density Function**

Many communication problems involve deterministic signals embedded in random noise. The simplest such combination of signal and noise is that of a constant frequency sinusoid added to narrow-band Gaussian noise. In the 1940s, Steven Rice analyzed this combination and published his results in the paper *Statistical Properties of a Sine-wave Plus Random Noise*, Bell System Technical Journal, **27**, pp. 109-157, January 1948. His work is outlined in this section.

Consider the sinusoid

$$s(t) = A_0 \cos(\omega_c t + \theta_0) = A_0 \cos\theta_0 \cos\omega_c t - A_0 \sin\theta_0 \sin\omega_c t\,, \tag{9-41}$$

where $A_0$, $\omega_c$, and $\theta_0$ are known constants. To signal s(t) we add noise $\eta(t)$ given by (9-1), a zero-mean WSS band-pass process with power $\sigma^2 = E[\eta^2] = E[\eta_c^2] = E[\eta_s^2]$. This sum of signal and noise can be written as

$$\begin{aligned} s(t) + \eta(t) &= [A_0 \cos\theta_0 + \eta_c(t)]\cos\omega_c t - [A_0 \sin\theta_0 + \eta_s(t)]\sin\omega_c t \\ &= \Gamma_2(t)\cos[\omega_c t + \varphi_2]\,, \end{aligned} \tag{9-42}$$

where

$$\Gamma_2(t) = \sqrt{[A_0 \cos\theta_0 + \eta_c(t)]^2 + [A_0 \sin\theta_0 + \eta_s(t)]^2}$$
$$\varphi_2(t) = \tan^{-1}\left[\frac{A_0 \sin\theta_0 + \eta_s(t)}{A_0 \cos\theta_0 + \eta_c(t)}\right], \quad -\pi < \varphi_2 \le \pi, \tag{9-43}$$

are the envelope and phase, respectively, of the signal+noise process. Note that the quantity $(A_0/\sqrt{2}\,)^2/\sigma^2$ is the signal-to-noise ratio, a ratio of powers.

Equation (9-43) represents a transformation from the components $\eta_c$ and $\eta_s$ into the envelope $\Gamma_2$ and phase $\varphi_2$. The inverse of this transformation is given by

$$\eta_c(t) = \Gamma_2(t)\cos\varphi_2(t) - A_0\cos\theta_0$$
$$\eta_s(t) = \Gamma_2(t)\sin\varphi_2(t) - A_0\sin\theta_0\,. \tag{9-44}$$

Note that constants $A_0\cos\theta_0$ and $A_0\sin\theta_0$ only influence the mean of $\eta_c$ and $\eta_s$. In the remainder of this section, we describe the statistical properties of envelope $\Gamma_2$ and phase $\varphi_2$.

At the same time t, processes $\eta_c(t)$ and $\eta_s(t)$ are statistically independent (however, for $\tau \neq 0$, $\eta_c(t)$ and $\eta_s(t+\tau)$ may be dependent). Hence, for $\eta_c(t)$ and $\eta_s(t)$ we can write the joint density

$$f(\eta_c, \eta_s) = \frac{\exp[-(\eta_c{}^2 + \eta_s{}^2)/2\sigma^2]}{2\pi\sigma^2} \tag{9-45}$$

(we choose to abuse notation for our convenience: $\eta_c$ and $\eta_s$ are used to denote both random processes and, as in (9-45), algebraic variables).

The joint density $f(\Gamma_2, \varphi_2)$ can be found by transforming (9-45). To accomplish this, the Jacobian

$$\frac{\partial(\eta_c,\eta_s)}{\partial(\Gamma_2,\varphi_2)}=\begin{bmatrix}\cos\varphi_2 & -\Gamma_2\sin\varphi_2\\ \sin\varphi_2 & \Gamma_2\cos\varphi_2\end{bmatrix} \tag{9-46}$$

can be used to write the joint density

$$f(\Gamma_2,\varphi_2)=f(\eta_c,\eta_s)\left|\det\frac{\partial(\eta_c,\eta_s)}{\partial(\Gamma_2,\varphi_2)}\right|_{\substack{\eta_c=\Gamma_2\cos\varphi_2-A_0\cos\theta_0\\ \eta_s=\Gamma_2\sin\varphi_2-A_0\sin\theta_0}} \tag{9-47}$$

$$f(\Gamma_2,\varphi_2)=\frac{\Gamma_2}{2\pi\sigma^2}\exp\left\{-\frac{1}{2\sigma^2}[{\Gamma_2}^2-2A_0\Gamma_2\cos(\varphi_2-\theta_0)+{A_0}^2]\right\}U(\Gamma_2)\,.$$

Now, the marginal density $f(\Gamma_2)$ can be found by integrating out the $\varphi_2$ variable to obtain

$$\begin{aligned}f(\Gamma_2)&=\int_0^{2\pi}f(\Gamma_2,\varphi_2)\,d\varphi_2\\ &=\frac{\Gamma_2}{\sigma^2}\exp\left\{-\frac{1}{2\sigma^2}[{\Gamma_2}^2+{A_0}^2]\right\}U(\Gamma_2)\frac{1}{2\pi}\int_0^{2\pi}\exp\{\frac{A_0\Gamma_2}{\sigma^2}\cos(\varphi_2-\theta_0)\}d\varphi_2\,.\end{aligned} \tag{9-48}$$

This result can be written by using the tabulated function

$$I_0(\beta)\equiv\frac{1}{2\pi}\int_0^{2\pi}\exp\{\beta\cos(\theta)\}d\theta\,, \tag{9-49}$$

the *modified Bessel function of order zero*. Now, use definition (9-49) in (9-48) to write

$$f(\Gamma_2)=\frac{\Gamma_2}{\sigma^2}I_0\left(\frac{\Gamma_2A_0}{\sigma^2}\right)\exp\left\{-\frac{1}{2\sigma^2}[{\Gamma_2}^2+{A_0}^2]\right\}U(\Gamma_2)\,, \tag{9-50}$$

a result known as the *Rice* probability density. As expected, $\theta_0$ does not enter into $f(\Gamma_2)$.

Equation (9-50) is an important result. It is the density function that statistically

describes the envelope $\Gamma_2$ at time t; for various values of $A_0/\sigma$, the function $\sigma f(\Gamma_2)$ is plotted on Figure 9-8 (the quantity $(A_0/\sqrt{2})^2/\sigma^2$ is the signal-to-noise ratio). For $A_0/\sigma = 0$, the case of no sinusoid, only noise, the density is Rayleigh. For large $A_0/\sigma$ the density becomes Gaussian. To observe this asymptotic behavior, note that for large $\beta$ the approximation

$$I_0(\beta) \approx \frac{e^{\beta}}{\sqrt{2\pi\beta}}, \quad \beta >> 1, \tag{9-51}$$

becomes valid. Hence, for large $\Gamma_2 A_0/\sigma^2$ Equation (9-50) can be approximated by

$$f(\Gamma_2) \approx \sqrt{\frac{\Gamma_2}{2\pi A_0 \sigma^2}} \exp\left\{-\frac{1}{2\sigma^2}[\Gamma_2 - A_0]^2\right\} U(\Gamma_2). \tag{9-52}$$

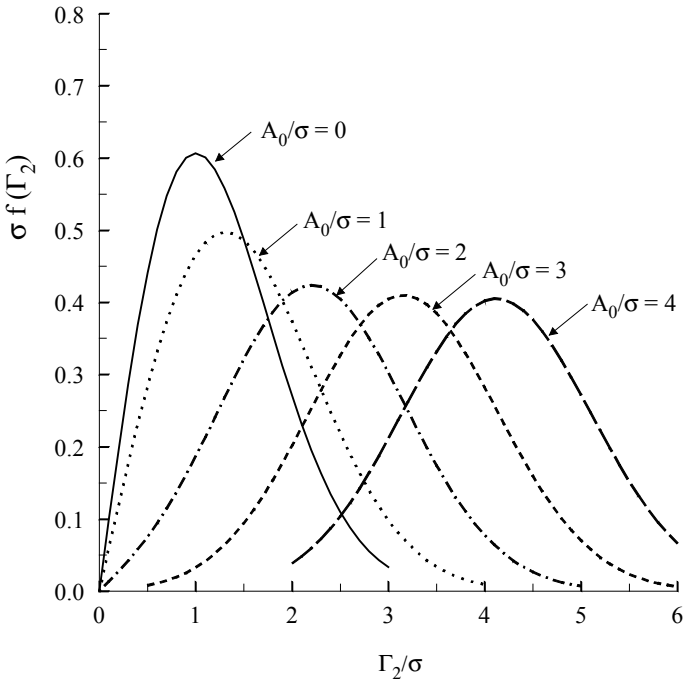


**Figure 9-8**: *Rice* density function for sinusoid plus noise. Plots are given for several values of $A_0/\sigma$. Note that f is approximately Rayleigh for small, positive $A_0/\sigma$; density f is approximately Gaussian for large $A_0/\sigma$.

For $A_0 >> \sigma$, this function has a very sharp peak at $\Gamma_2 = A_0$, and it falls off rapidly from its peak value. Under these conditions, the approximation

$$f(\Gamma_2) \approx \frac{1}{\sqrt{2\pi\sigma^2}} \exp\left\{-\frac{1}{2\sigma^2}[\Gamma_2 - A_0]^2\right\} \tag{9-53}$$

holds for values of $\Gamma_2$ near $A_0$ (*i.e.*, $\Gamma_2 \approx A_0$) where $f(\Gamma_2)$ is significant. Hence, for large $A_0/\sigma$, envelope $\Gamma_2$ is approximately Gaussian distributed.

The marginal density $f(\varphi_2)$ can be found by integrating $\Gamma_2$ out of (9-47). Before integrating, complete the square in $\Gamma_2$, and express (9-47) as

$$f(\Gamma_2, \varphi_2) = \frac{\Gamma_2}{2\pi\sigma^2} \exp\left\{-\frac{1}{2\sigma^2}[\Gamma_2 - A_0\cos(\varphi_2 - \theta_0)]^2\right\} \exp\left\{-\frac{A_0^2}{2\sigma^2}\sin^2(\varphi_2 - \theta_0)\right\} U(\Gamma_2). \tag{9-54}$$

Now, integrate $\Gamma_2$ out of (9-54) to obtain

$$\begin{aligned} f(\varphi_2) &= \int_0^\infty f(\Gamma_2, \varphi_2) d\Gamma_2 \\ &= \exp\left\{-\frac{A_0^2}{2\sigma^2}\sin^2(\varphi_2 - \theta_0)\right\} \int_0^\infty \frac{\Gamma_2}{2\pi\sigma^2} \exp\left\{-\frac{1}{2\sigma^2}[\Gamma_2 - A_0\cos(\varphi_2 - \theta_0)]^2\right\} d\Gamma_2 . \end{aligned} \tag{9-55}$$

On the right-hand-side of (9-55), the integral can be expressed as the two integrals

$$\begin{aligned} &\int_0^\infty \frac{\Gamma_2}{2\pi\sigma^2} \exp\left\{-\frac{1}{2\sigma^2}[\Gamma_2 - A_0\cos(\varphi_2 - \theta_0)]^2\right\} d\Gamma_2 \\ &= \int_0^\infty \frac{2\{\Gamma_2 - A_0\cos(\varphi_2 - \theta_0)\}}{4\pi\sigma^2} \exp\left\{-\frac{1}{2\sigma^2}[\Gamma_2 - A_0\cos(\varphi_2 - \theta_0)]^2\right\} d\Gamma_2 \\ &\quad + \frac{A_0\cos(\varphi_2 - \theta_0)}{2\pi\sigma^2} \int_0^\infty \exp\left\{-\frac{1}{2\sigma^2}[\Gamma_2 - A_0\cos(\varphi_2 - \theta_0)]^2\right\} d\Gamma_2 \end{aligned} \tag{9-56}$$

After a change of variable $\nu = [\Gamma_2 - A_0\cos(\varphi_2 - \theta_0)]^2$, the first integral on the right-hand-side of (9-56) can be expressed as

$$\begin{aligned}
&\int_0^{\infty} \frac{2\{\Gamma_2 - A_0\cos(\varphi_2 - \theta_0)\}}{4\pi\sigma^2} \exp\left\{-\frac{1}{2\sigma^2}[\Gamma_2 - A_0\cos(\varphi_2 - \theta_0)]^2\right\} d\Gamma_2 \\
&\quad = \frac{1}{4\pi\sigma^2}\int_{A_0^2\cos^2(\varphi_2-\theta_0)}^{\infty} \exp[-\frac{\upsilon}{2\sigma^2}]d\nu \qquad (9\text{-}57) \\
&\quad = \frac{1}{2\pi}\exp\left[-\frac{A_0^2\cos^2(\varphi_2-\theta_0)}{2\sigma^2}\right].
\end{aligned}$$

After a change of variable $\nu = [\Gamma_2 - A_0\cos(\varphi_2 - \theta_0)]/\sigma$, the second integral on the right-hand-side of (9-56) can be expressed as

$$\begin{aligned}
&\frac{1}{\sqrt{2\pi}\sigma}\int_0^{\infty} \exp\left\{-\frac{1}{2\sigma^2}[\Gamma_2 - A_0\cos(\varphi_2 - \theta_0)]^2\right\} d\Gamma_2 \\
&\quad = \frac{1}{\sqrt{2\pi}}\int_{-(A_0/\sigma)\cos[\varphi_2-\theta_0]}^{\infty} \exp\left\{-\tfrac{1}{2}\nu^2\right\} d\nu \qquad (9\text{-}58) \\
&\quad = 1 - \frac{1}{\sqrt{2\pi}}\int_{-\infty}^{-(A_0/\sigma)\cos[\varphi_2-\theta_0]} \exp\left\{-\tfrac{1}{2}\nu^2\right\} d\nu \\
&\quad = F(\frac{A_0}{\sigma}\cos[\varphi_2 - \theta_0]),
\end{aligned}$$

where

$$F(x) \equiv \frac{1}{\sqrt{2\pi}}\int_{-\infty}^{x} \exp\left[-\frac{\nu^2}{2}\right] d\nu$$

is the distribution function for a zero-mean, unit variance Gaussian random variable (the identity F(-x) = 1 - F(x) was used to obtain (9-58)).

Finally, we are in a position to write $f(\varphi_2)$, the density function for the instantaneous phase. This density can be written by using (9-57) and (9-58) in (9-55) to write

$$f(\varphi_2) = \frac{1}{2\pi}\exp\left[-\frac{A_0^2}{2\sigma^2}\right] + \frac{A_0\cos(\varphi_2-\theta_0)}{\sqrt{2\pi}\sigma}\exp\left\{-\frac{A_0^2}{2\sigma^2}\sin^2(\varphi_2-\theta_0)\right\}F\left(\frac{A_0}{\sigma}\cos[\varphi_2-\theta_0]\right), \quad (9\text{-}59)$$

the density function for the phase of a sinusoid embedded in narrow-band noise. For various values of SNR and for $\theta_0 = 0$, density $f(\varphi_2)$ is plotted on Fig. 9-9. For a SNR of zero (*i.e.*, $A_0 = 0$), the phase is uniform. As SNR $A_0^2/\sigma^2$ increases, the density becomes more sharply peaked (in general, the density will peak at $\theta_0$, the phase of the sinusoid). As SNR $A_0^2/\sigma^2$ approaches infinity, the density of the phase approaches a delta function at $\theta_0$.

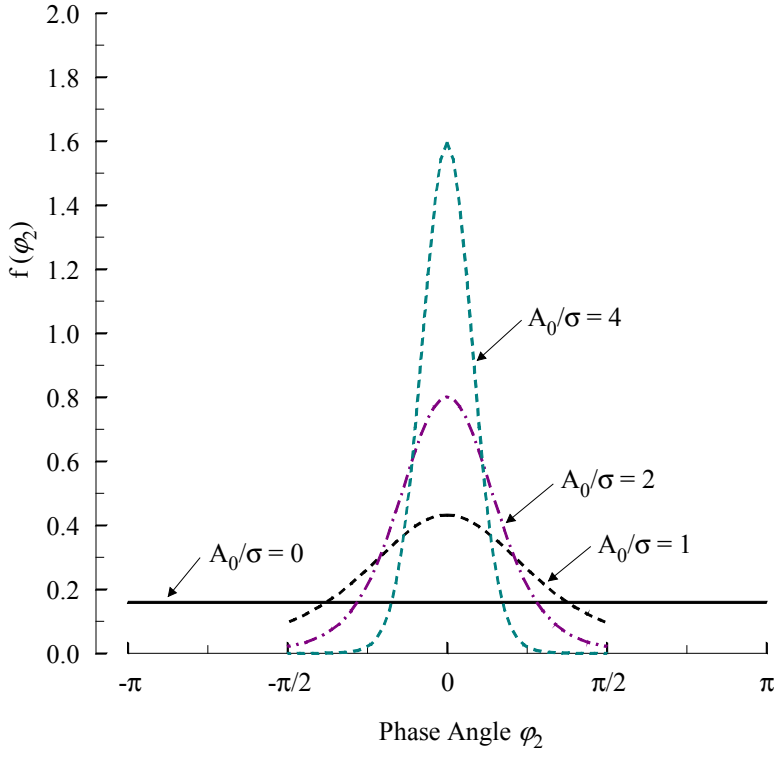


**Figure 9-9:** Density function for phase of signal plus noise $A_0\cos(\omega_0 t+\theta_0)$ + $\{\eta_c(t)\cos(\omega_0 t) - \eta_s(t)\sin(\omega_0 t)\}$ for the case $\theta_0 = 0$.

**Shot Noise**

*Shot noise* results from filtering a large number of independent and randomly-occuring-in-time impulses. For example, in a temperature-limited vacuum diode, independent electrons reach the anode at independent times to produce a shot noise process in the diode output circuit. A similar phenomenon occurs in diffusion-limited *pn* junctions. To understand shot noise, you must first understand Poisson point processes and Poisson impulses.

Recall the definition and properties of the Poissson point process that was discussed in Chapters 2 and 7 (also, see Appendix 9-B). The Poisson points occur at times $t_i$ with an average density of $\lambda_d$ points per unit length. In an interval of length $\tau$, the number of points is distributed with a Poisson density with parameter $\lambda_d\tau$.

Use this Poisson process to form a sequence of *Poisson Impulses*, a sequence of impulses located at the Poisson points and expressed as

$$z(t) = \sum_i \delta(t - t_i), \tag{9-60}$$

where the $t_i$ are the Poisson points. Note that z(t) is a generalized random process; like the delta function, it can only be characterized by its behavior under an integral sign. When z(t) is integrated, the result is the Poisson random process

$$x(t) = \int_0^t z(\tau)d\tau = \begin{cases} \mathbf{n}(0,t), & t > 0 \\ 0, & t = 0 \\ -\mathbf{n}(0,t) & t < 0, \end{cases} \tag{9-61}$$

where $\mathbf{n}(t_1,t_2)$ is the number of Poisson points in the interval $(t_1,t_2)$. Likewise, by passing the Poisson process x(t) through a generalized differentiator (as illustrated by Fig. 9-10), it is possible to obtain z(t).

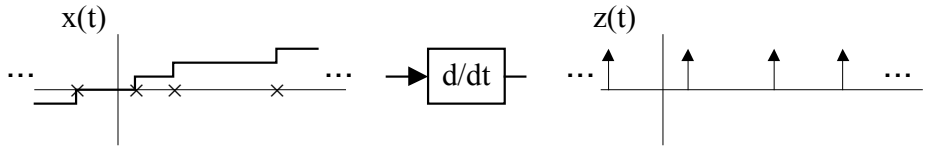


**Figure 9-10:** Differentiate the Poisson Process to get Poisson impulses.

The mean of z(t) is simply the derivative of the mean value of x(t). Since $E[x(t)]=\lambda_d t$, we can write

$$\eta_z = E[z(t)] = \frac{d}{dt} E[x(t)] = \lambda_d . \tag{9-62}$$

This formal result needs a physical interpretation. One possible interpretation is to view $\eta_z$ as

$$\eta_z = \lim_{t\to\infty} \frac{1}{t}\int_{-t/2}^{t/2} z(\tau)d\tau = \lim_{t\to\infty} \frac{1}{t}\left(\lambda_d t + \text{ random fluctuation with increasing t }\right) = \lambda_d . \tag{9-63}$$

For large t, the integral in (9-63) fluctuates around mean $\lambda_d t$ with a variance of $\lambda_d t$ (both the mean and variance of the number of Poisson points in (-t/2, t/2) is $\lambda_d t$). But, the integral is multiplied by 1/t; the product has a mean of $\lambda_d$ and a variance like $\lambda_d/t$. Hence, as t becomes large, the random temporal fluctuations become insignificant compared to $\lambda_d$, the infinite-time-interval average $\eta_z$.

Important correlations involving z(t) can be calculated easily. Because $R_x(t_1,t_2) = \lambda_d^2 t_1 t_2 + \lambda_d \min(t_1,t_2)$ (see Chapter 7), we obtain

$$\begin{aligned} R_{xz}(t_1,t_2) &= \frac{\partial}{\partial t_2} R_x(t_1,t_2) = \lambda_d^2 t_1 + \lambda U(t_1 - t_2) \\ R_z(t_1,t_2) &= \frac{\partial}{\partial t_1} R_{zx}(t_1,t_2) = \lambda_d^2 + \lambda_d \delta(t_1 - t_2) . \end{aligned} \tag{9-64}$$

The Fourier transform of $R_z(\tau)$ yields

$$\boldsymbol{S}_z(\omega) = \lambda_d + 2\pi\,\lambda_d^2\,\delta(\omega)\,, \tag{9-65}$$

the power spectrum of the Poisson impulse process.

Let h(t) be a real-valued function of time and define

$$s(t) = \sum_i h(t - t_i)\,, \tag{9-66}$$

a sum known as *shot noise*. The basic idea here is illustrated by Fig. 9-11. A sequence of δ functions described by (9-60) (*i.e.*, process z(t)) is input to system h(t) to form output shot noise process s(t). The idea is simple: process s(t) is the output of a system activated by a sequence of impulses (that model electrons arriving at an anode, for example) that occur at the random Poisson points $t_i$.

Determined easily are the elementary properties of shot noise s(t). Using the method discussed in Chapter 7, we obtain the mean

$$\eta_s = E[s(t)] = E[z(t) * h(t)] = h(t) * E[z(t)] = \lambda_d \int_0^\infty h(t)dt = \lambda_d H(0)\,. \tag{9-67}$$

Shot noise s(t) has the power spectrum

$$\boldsymbol{S}_s(\omega) = |H(\omega)|^2\,\boldsymbol{S}_z(\omega) = 2\pi\lambda_d^2\,H^2(0)\delta(\omega) + \lambda_d\,|H(\omega)|^2 = 2\pi\eta_s^2\,\delta(\omega) + \lambda_d\,|H(\omega)|^2\,. \tag{9-68}$$

Finally, the autocorrelation is

$$R_s(\tau) = \mathcal{F}^{-1}[\boldsymbol{S}_s(\omega)] = \lambda_d^2\,H^2(0) + \frac{\lambda_d}{2\pi}\int_{-\infty}^{\infty}|H(\omega)|^2 e^{j\omega\tau}d\omega = \lambda_d^2\,H^2(0) + \lambda_d\,\rho(\tau)\,, \tag{9-69}$$

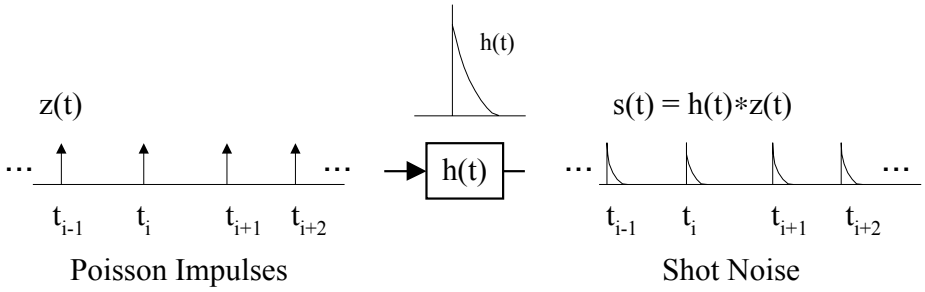


**Figure 9-11:** Converting Poisson impulses z(t) into shot noise s(t)

where

$$\rho(\tau) = \frac{1}{2\pi}\int_{-\infty}^{\infty} |H(\omega)|^2 e^{j\omega\tau} d\omega = \int_{-\infty}^{\infty} h(t)h(t+\tau)dt\,. \tag{9-70}$$

From (9-67) and (9-69), shot noise has a mean and variance of

$$\begin{aligned} \eta_s &= \lambda_d H(0) \\ \sigma_s^2 &= [\lambda_d^2 H^2(0) + \lambda_d \rho(0)] - [\lambda_d H(0)]^2 = \lambda_d \rho(0) = \frac{\lambda_d}{2\pi}\int_{-\infty}^{\infty} |H(\omega)|^2 \, d\omega\,, \end{aligned} \tag{9-71}$$

respectively (Equation (9-71) is known as *Campbell's Theorem*).

**Example**: Let $h(t) = e^{-\beta t}U(t)$ so that $H(\omega) = 1/(\beta + j\omega)$, $\rho(t) = e^{-\beta|t|}/2\beta$ and

$$\begin{aligned} \eta_s = E[s(t)] &= \frac{\lambda_d}{\beta} & R_s(\tau) &= \frac{\lambda_d}{2\beta} e^{-\beta|\tau|} + \left[\frac{\lambda_d}{\beta}\right]^2 \\ \sigma_s^2 &= \frac{\lambda_d}{2\beta} & \boldsymbol{S}_s(\omega) &= 2\pi\left[\frac{\lambda_d}{\beta}\right]^2 \delta(\omega) + \frac{\lambda_d}{\beta^2 + \omega^2} \end{aligned} \tag{9-72}$$

**First-Order Density Function for Shot Noise**

In general, the first-order density function $f_s(x;t)$ that describes shot noise s(t) cannot be calculated easily. Before tackling the difficult general case, we first consider a simpler special

case where it is assumed that h(t) is of finite duration T. That is, we assume initially that

$$h(t) = 0, \qquad t < 0 \text{ and } t > T. \tag{9-73}$$

Because of (9-73), shot noise s at time t depends only on the Poisson impulses in the interval (t - T, t). Let random variable $\mathbf{n_T}$ denote the number of Poisson impulses during (t - T, t). From Chapter 1, we know that

$$\mathbf{P}[\mathbf{n_T} = k] = e^{-\lambda_d T}\frac{(\lambda_d T)^k}{k!}. \tag{9-74}$$

Now, the Law of Total Probability (see Ch. 1 and Ch. 2 of these notes) can be applied to write the first-order density function of the shot noise process s(t) as

$$f_s(x) = \sum_{k=0}^{\infty} f_s(x\,|\,\mathbf{n_T} = k)\mathbf{P}[\mathbf{n_T} = k] = \sum_{k=0}^{\infty} f_s(x\,|\,\mathbf{n_T} = k)e^{-\lambda_d T}\frac{(\lambda_d T)^k}{k!} \tag{9-75}$$

(note that $f_s(x)$ is independent of absolute time t). We must find $f_s(x\,|\,\mathbf{n_T} = k)$, the density of shot noise s(t) conditioned on there being exactly k Poisson impulses in the interval (t - T, t).

From our previous study of Poisson points (see Chapters 1 and 7), we know that the impulses are distributed randomly and independently on (t - T, t). That is, the impulse locations are k independent random variables, each of which is uniformly distributed on (t - T, t).

For the case k = 1, at any fixed time t, $f_s(x\,|\,\mathbf{n_T} = 1)$ is actually equal to the density $g_1(x)$ of the random variable

$$x_1(t) \equiv h(t - t_1), \tag{9-76}$$

where random variable $t_1$ is uniformly distributed on (t - T, t). That is, $g_1(x) \equiv f_s(x \mid \mathbf{n_T} = 1)$ describes the result that is obtained by transforming a uniform density (used to describe $t_1$) by the transformation $h(t - t_1)$.

Convince yourself that density $g_1(x) = f_s(x \mid \mathbf{n_T} = 1)$ does not depend on time. Note that for any given time t, random variable $t_1$ is uniform on (t-T, t), and $x_1(t) \equiv h(t-t_1)$ is assigned values in the set $\{h(\alpha) : 0 < \alpha < T\}$, the assignment not depending on t. Hence, density $g_1(x) \equiv f_s(x \mid \mathbf{n_T} = 1)$ does not depend on t.

The density $f_s(x \mid \mathbf{n_T} = 2)$ can be found in a similar manner. Let $t_1$ and $t_2$ denote independent random variables, each of which is uniformly distributed on (t - T, t), and define

$$x_2(t) \equiv h(t-t_1) + h(t-t_2). \tag{9-77}$$

At fixed time t, the random variable $x_2(t)$ is described by the density $f_s(x \mid \mathbf{n_T} = 2) = g_1 * g_1$ (*i.e.,* the convolution of $g_1$ with itself) since $h(t - t_1)$ and $h(t - t_2)$ are independent and identically distributed with density $g_1$.

The general case $f_s(x \mid \mathbf{n_T} = k)$ is similar. At fixed time t, the density that describes

$$x_k(t) \equiv h(t-t_1) + h(t-t_2) + \cdots + h(t-t_k) \tag{9-78}$$

is

$$g_k(x) \equiv f_s(x \mid \mathbf{n_T} = k) = \underbrace{g_1(x) * g_1(x) * \cdots * g_1(x)}_{\text{k convolutions}}, \tag{9-79}$$

the density $g_1$ convolved with itself k times.

The desired density can be expressed in terms of results given above. Simply substitute (9-79) into (9-75) and obtain

$$f_s(x) = e^{-\lambda_d T} \sum_{k=0}^{\infty} g_k(x) \frac{(\lambda_d T)^k}{k!}. \tag{9-80}$$

When $\mathbf{n_T} = 0$, there are no Poisson points in (t - T, t), and we have

$$g_0(x) \equiv f_s(x \,|\, \mathbf{n_T} = 0) = \delta(x) \tag{9-81}$$

since the output is zero. Convergence is fast, and (9-80) is useful for computing the density $f_s$ when $\lambda_d T$ is small (the case for *low density* shot noise), say on the order of 1, so that, on the average, there are only a few Poisson impulses in the interval (t - T, t). For the case of *low density* shot noise, (9-80) cannot (in general) be approximated by a Gaussian density.

**$f_s(x)$ For An Infinite Duration h(t)**

The first-order density function $f_s(x)$ is much more difficult to calculate for the general case where h(t) is of infinite duration (not subject to the restriction (9-73)). We show *that shot noise is approximately Gaussian distributed when* $\lambda_d$ *is large compared to the time interval over which* h(t) *is significant* (so that, on the average, many Poisson impulses are filtered to form s(t)).

To establish this fact, consider first a finite duration interval (-T/2, T/2), and let random variable $\mathbf{n}_T$, described by (9-74), denote the number of Poisson impulses that are contained in the interval. Also, define the *time-limited shot noise*

$$s_T(t) \equiv \sum_{k=1}^{\mathbf{n_T}} h(t - t_k), \quad -T/2 < t < T/2, \tag{9-82}$$

where the identically distributed and independent random variables $t_i$ denote the times at which the Poisson impulses occur in the interval (each $t_i$ is uniformly distributed on the interval). Shot noise s(t) is the limit of $s_T(t)$ as T approaches infinity.

In our analysis of s(t), we first consider the characteristic function

$$\Phi_S(\omega) = E\left[e^{j\omega s}\right] = \lim_{T\to\infty} E\left[e^{j\omega s_T}\right]. \tag{9-83}$$

Now, write the characteristic function of $s_T$ as

$$E\left[e^{j\omega s_T}\right] = \sum_{k=0}^{\infty} E\left[e^{j\omega s_T} \,|\, \mathbf{n_T} = k\right] \mathbf{P}\left[\mathbf{n_T} = k\right], \tag{9-84}$$

where $\mathbf{P}[\mathbf{n_T} = k]$ is given by (9-74). In the interval (-T/2, T/2), the locations of the $\mathbf{n_T}$ Poisson impulses are identically and independently distributed. Hence, the terms $h(t - t_i)$ in $s_T(t)$ (see (9-82)) are independent so that

$$E\left[e^{j\omega s_T} \,|\, \mathbf{n_T} = k\right] = \left(E\left[e^{j\omega s_T} \,|\, \mathbf{n_T} = 1\right]\right)^k, \tag{9-85}$$

where

$$E\left[e^{j\omega s_T} \,|\, \mathbf{n_T} = 1\right] = \frac{1}{T}\int_{-T/2}^{T/2} e^{j\omega h(t-x)} dx, \qquad -T/2 < t < T/2, \tag{9-86}$$

since each $t_i$ is uniformly distributed on (-T/2, T/2). Finally, by using (9-83) through (9-86), we can write

$$\Phi_s(\omega) = \lim_{T\to\infty} E\left[e^{j\omega s_T}\right] = \lim_{T\to\infty} \sum_{k=0}^{\infty} E\left[e^{j\omega s_T} \,|\, \mathbf{n_T} = k\right] \mathbf{P}\left[\mathbf{n_T} = k\right]$$

$$= \lim_{T\to\infty} \sum_{k=0}^{\infty} \left(\frac{1}{T}\int_{-T/2}^{T/2} e^{j\omega h(t-x)}dx\right)^k e^{-\lambda_d T}\frac{(\lambda_d T)^k}{k!} \tag{9-87}$$

$$= \lim_{T\to\infty} e^{-\lambda_d T} \sum_{k=0}^{\infty} \frac{\left(\lambda_d \int_{-T/2}^{T/2} e^{j\omega h(t-x)}dx\right)^k}{k!}.$$

Recalling the Taylor series of the exponential function, we can write (9-87) as

$$\Phi_s(\omega) = \lim_{T\to\infty} \exp\{-\lambda_d T\} \exp\left(\lambda_d \int_{-T/2}^{T/2} e^{j\omega h(t-x)}dx\right) = \exp\left[\lambda_d \int_{-\infty}^{\infty} \left(e^{j\omega h(t-x)} - 1\right)dx\right], \tag{9-88}$$

a general formula for the characteristic function of the shot noise process.

In general, Equation (9-88) is impossible to evaluate in closed form. However, this formula can be used to show that shot noise is approximately Gaussian distributed when $\lambda_d$ is large compared to the time constants in h(t) (*i.e.*, compared to the time duration where h(t) is significant). First, this task will be made simpler if we standardize s(t) to

$$s(t) \equiv \frac{s(t) - \lambda_d H(0)}{\sqrt{\lambda_d}}, \tag{9-89}$$

so that

$$\begin{aligned} &E[s] = 0 \\ &R_s(\tau) = \rho(\tau) = \int_{-\infty}^{\infty} h(t)h(t+\tau)dt \end{aligned}. \tag{9-90}$$

(see (9-67) and (9-69)). The characteristic functions of $s$ and s are related by

$$\Phi_s(\omega) = E\left[e^{j\omega s}\right] = E\left[\exp\left[j\omega\frac{s - \lambda_d H(0)}{\sqrt{\lambda_d}}\right]\right] = \exp\left[-j\omega\sqrt{\lambda_d}H(0)\right]\Phi_s(\omega/\sqrt{\lambda_d}). \tag{9-91}$$

Use (9-88) in (9-91) to write

$$\Phi_s(\omega) = \exp\left[\lambda_d\int_{-\infty}^{\infty}\left\{\exp\left[\frac{j\omega}{\sqrt{\lambda_d}}h(t-x)\right] - 1 - \frac{j\omega}{\sqrt{\lambda_d}}h(t-x)\right\}dx\right]. \tag{9-92}$$

Now, in the integrand, expand the exponential in a power series, and cancel out the zero and first-order terms to obtain

$$\Phi_s(\omega) = \exp\left[\lambda_d\int_{-\infty}^{\infty}\sum_{k=2}^{\infty}\frac{(j\omega)^k}{k!}\left\{\frac{h(t-x)}{\sqrt{\lambda_d}}\right\}^k dx\right] = \exp\left[\lambda_d\sum_{k=2}^{\infty}\frac{(j\omega)^k}{k!}\int_{-\infty}^{\infty}\left\{\frac{h(x)}{\sqrt{\lambda_d}}\right\}^k dx\right]. \tag{9-93}$$

Finally, assume that $\lambda_d$ is large compared to the time duration during which h(t) is significant. For example, this will be the case if the decay of h(t) (or the envelope of h(t)) is faster than a function of the form $c_m e^{-t/\tau_m}U(t)$, and $\lambda_d$ is large compared to the time constant $\tau_m$. This insures that, on the average and at any give time, shot noise s(t) results from the filtering of a large number of random Poisson impulses. For this case, only the first term in the sum is significant; for large $\lambda_d$, Equation (9-93) can be approximated as

$$\Phi_s(\omega) \approx \exp\left[\frac{(j\omega)^2}{2}\int_{-\infty}^{\infty}h^2(x)dx\right] = \exp\left[-\frac{1}{2}\sigma_s^2\omega^2\right], \tag{9-94}$$

where

$$\sigma_s^2 = R_s(0) \tag{9-95}$$

is the variance of standardized shot noise $s(t)$ (see (9-90)). Note that Equation (9-94) is the characteristic function of a zero-mean, Gaussian random variable with variance (9-95). Hence, *shot noise is approximately Gaussian distributed when* $\lambda_d$ *is large compared to the time interval over which* h(t) *is significant* (so that, on the average, a large number of Poisson impulses are filtered to form s(t)).

**Example: Temperature-Limited Vacuum Diode**

In classical communications system theory, a temperature-limited vacuum diode is the quintessential example of a shot noise generator (the phenomenon was first predicted and analyzed theoretically by Schottky in his 1918 paper: *Theory of Shot Effect*, Ann. Phys., Vol 57, Dec. 1918, pp. 541-568). In fact, over the years, noise generators (used for testing/aligning communication receivers, low noise preamplifiers, etc.) based on vacuum diodes (*i.e.,* Sylvania 5722 special purpose noise generator diode) have been offered on a commercial basis.

Vacuum noise generating diodes are operated in a *temperature-limited*, or *saturated*, mode. Essentially, all of the available electrons are collected by the plate (few return to the cathode) so that increasing plate voltage does not increase plate current (*i.e.,* the tube is *saturated*). The only way to increase plate current is to increase filament/cathode temperature. Under this condition, between electrons, space charge effects can be negligible so that individual electrons are, more or less, independent of each other.

The basic circuit is illustrated by Figure 9-12. In a random manner, electrons are emitted by the cathode, and they flow a distance *d* to the plate to form the current i(t). If emitted at t = 0, an independent electron contributes a current h(t), and the aggregate plate current is given by

$$i(t) = \sum_k h(t - t_k), \tag{9-96}$$

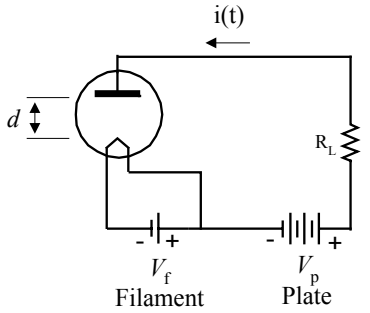


**Figure 9-12:** Temperature-limited vacuum diode used as a shot noise generator.

where $t_k$ are the Poisson-distributed independent times at which electrons are emitted by the cathode (see Equation (9-66)). In what follows, we approximate h(t).

As discussed above, space charge effects are negligible and the electrons are independent. Since there is no space charge between the cathode and plate, the potential distribution $V$ in this region satisfies Laplace's equation

$$\frac{\partial^2 V}{\partial^2 \mathrm{x}} = 0 . \tag{9-97}$$

The potential must satisfy the boundary conditions $V(0) = 0$ and $V(d) = V_p$. Hence, simple integration yields

$$V = \frac{V_p}{d}\mathrm{x} , \qquad 0 \le \mathrm{x} \le d . \tag{9-98}$$

As an electron flows from the cathode to the plate, its velocity and energy increase. At point x between the cathode and plate, the energy increase is given by

$$\mathrm{E_n}(\mathrm{x}) = eV(\mathrm{x}) = e\frac{V_p}{d}\mathrm{x} , \tag{9-99}$$

where $e$ is the basic electronic charge.

Power is the rate at which energy changes. Hence, the instantaneous power flowing from the battery into the tube is

$$\frac{dE_n}{dt} = \frac{dE_n}{dx}\frac{dx}{dt} = e\frac{V_p}{d}\frac{dx}{dt} = V_p\, h\,, \tag{9-100}$$

where h(t) is current due to the flow of a single electron (note that $d^{-1}$dx/dt has units of $\sec^{-1}$ so that $(e/d)$ dx/dt has units of charge/sec, or current). Equation (9-100) can be solved for current to obtain

$$h = \frac{e}{d}\frac{dx}{dt} = \frac{e}{d}v_x\,, \tag{9-101}$$

where $v_x$ is the instantaneous velocity of the electron.

Electron velocity can be found by applying Newton's laws. The force on an electron is just $e(V_p/d)$, the product of electronic charge and electric field strength. Since force is equal to the product of electron mass $m$ and acceleration $a_x$, we have

$$a_x = \frac{e}{m}\frac{V_p}{d}\,. \tag{9-102}$$

As it is emitted by the cathode, an electron has an initial velocity that is Maxwellian distributed. However, to simplify this example we will assume that the initial velocity is zero. With this assumption, electron velocity can be obtained by integrating (9-102) to obtain

$$v_x = \frac{e}{m}\frac{V_p}{d}t\,. \tag{9-103}$$

Over transition time $t_T$ the average velocity is

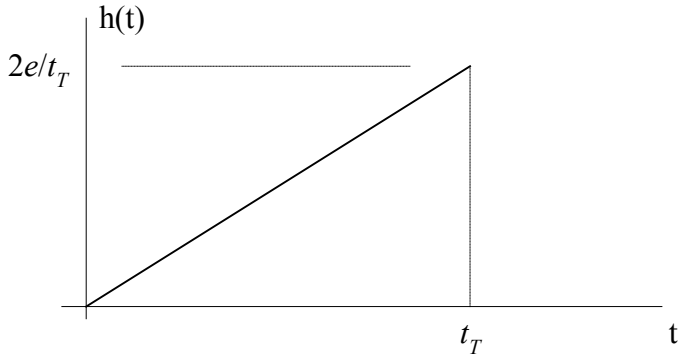


**Figure 9-13**: Current due to a single electron emitted by the cathode at t = 0.

$$\langle v_x \rangle = \frac{1}{t_T}\int_0^{t_T} v_x \, dt = \frac{e}{2m}\frac{V_p}{d}t_T = \frac{d}{t_T}. \tag{9-104}$$

Finally, combine these last two equations to obtain

$$v_x = \left(\frac{2d}{t_T^2}\right)t, \quad 0 \le t \le t_T . \tag{9-105}$$

With the aid of this last relationship, we can determine current as a function of time. Simply combine (9-101) and (9-105) to obtain

$$h(t) = \left(\frac{2e}{t_T^2}\right)t, \quad 0 \le t \le t_T , \tag{9-106}$$

the current pulse generated by a single electron as it travels from the cathode to the plate. This current pulse is depicted by Figure 9-13.

The bandwidth of shot noise s(t) is of interest. For example, we may use the noise generator to make relative measurements on a communication receiver, and we may require the noise spectrum to be "flat" (or "white") over the receiver bandwidth (the noise spectrum amplitude is not important since we are making relative measurements). To a certain "flatness",

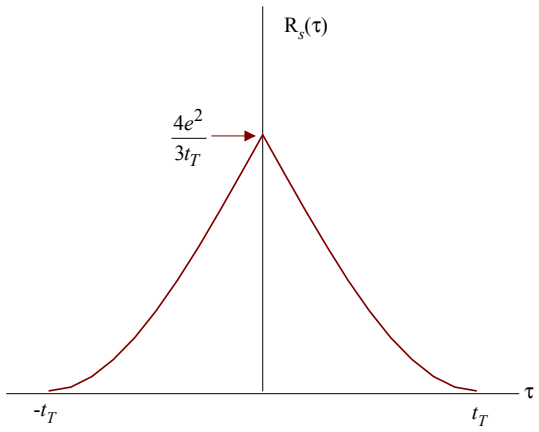


**Figure 9-14:** Autocorrelation function of normalized shot noise process.

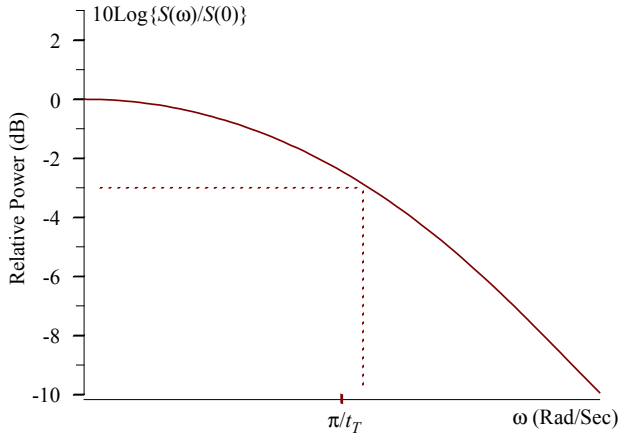


**Figure 9-15:** Relative power spectrum of normalized shot noise process.

we can compute and examine the power spectrum of standardized $s(t)$ described by (9-89). As given by (9-90), the autocorrelation of $s(t)$ is

$$\begin{aligned} R_s(\tau) &= \left(2\frac{e}{t_T}\right)^2 \int_0^{t_T-\tau} t(t+\tau)dt = \frac{4}{3}\frac{e^2}{t_T}\left(1-\frac{\tau}{t_T}\right)^2\left(1+\frac{\tau}{2t_T}\right), \quad 0 \le \tau \le t_T \\ &= R_s(-\tau), \qquad -t_T \le \tau \le 0. \\ &= 0, \qquad \text{otherwise} \end{aligned} \tag{9-107}$$

The power spectrum of $s(t)$ is the Fourier transform of (9-107), a result given by

$$S(\omega) = 2\int_0^\infty R_s(\tau)\cos(\omega\tau)d\tau = \frac{4}{(\omega t_T)^4}\left((\omega t_T)^2 + 2(1-\cos\omega t_T - \omega t_T \sin\omega t_T)\right). \tag{9-108}$$

Plots of the autocorrelation and relative power spectrum (plotted in dB relative to peak power at $\omega = 0$) are given by Figures 9-14 and 9-15, respectively.

To within 3dB, the power spectrum is "flat" from DC to a little over $\omega = \pi/t_T$. For the Sylvania 5722 noise generator diode, the cathode-to-plate spacing is .0375 inches and the transit time is about $3\times10^{-10}$ seconds. For this diode, the 3dB cutoff would be about $1/2t_T$ = 1600Mhz. In practical application, where electrode/circuit stray capacitance/inductance limits frequency

range, the Sylvania 5722 has been used in commercial noise generators operating at over 400Mhz.